

# Extraction and Detection of DNA from *Bacillus anthracis* Spores and the Vegetative Cells within 1 min

Kadir Aslan,<sup>†</sup> Michael J. R. Previte,<sup>†</sup> Yongxia Zhang,<sup>†</sup> Theresa Gallagher,<sup>‡</sup> Les Baillie,<sup>§</sup> and Chris D. Geddes<sup>\*†</sup>

Institute of Fluorescence, Laboratory for Advanced Medical Plasmonics and Laboratory for Advanced Fluorescence Spectroscopy, Medical Biotechnology Center, and Biodefense Initiative, Medical Biotechnology Center, University of Maryland Biotechnology Institute, 725 West Lombard Street, Baltimore, Maryland 21201, and Welsh School of Pharmacy, Cardiff University, King Edward VII Avenue, Cardiff CF10 3NB, Cardiff, Wales U.K.

The use of a combination of low-cost technologies to both extract and detect anthrax DNA from spores and vegetative cells in two steps within 1 min is described. In a cavity, microwave energy is highly focused using thin-film aluminum “bow-tie” structures, to extract DNA from whole spores within 20 s. The detection of the released DNA, from less than 1000 vegetative cells, without additional preprocessing steps is accomplished in an additional 30 s by employing the microwave-accelerated metal-enhanced fluorescence technique. The new platform technology presented here is a highly attractive alternative method for DNA extraction and the fast detection of Gram-positive bacteria and potentially other pathogenic species and cells as well.

*Bacillus anthracis*, the bacterium that causes anthrax, is a pathogen of mammals that persists outside of an infected host as an inert spore. Following uptake by a susceptible species, the spore converts to a biologically active form known as the vegetative organism, which produces a range of toxins and replicates within the blood of the host.<sup>1</sup> In mammals, the disease usually runs a hyperacute course in which signs of illness can be absent until shortly before death and is thought to be caused by a combination of toxin-mediated immune suppression and massive terminal bacteremia.<sup>2</sup> Consequently, early diagnosis and treatment of anthrax is essential because the disease reaches a point at which antibiotics are no longer effective due to the accumulation of lethal levels of toxin.<sup>3</sup> Thus, the ability to rapidly detect the presence of both the spore and vegetative forms of the organism in clinical samples would enable clinicians to instigate timely therapeutic intervention.

At present, the rapid detection of *B. anthracis* spores, the form of the organism most likely to be encountered during a biological

terror attack, is based on the recognition of specific markers on the spore surface or nucleic acid (DNA) sequestered within the body of the spore. The spore is constructed inside a vegetative bacterium and upon release is covered with cellular debris derived from this mother cell comprising cellular proteins, carbohydrates and DNA.<sup>4</sup> Polymerase chain reaction (PCR) has been used to detect specific DNA-encoded targets derived from the mother cell on the surface of unprocessed *B. anthracis* spores within 2 h, with a sensitivity limit of 10<sup>2</sup> spores per reaction.<sup>5,6</sup>

Our research group recently reported a technique called microwave-accelerated metal-enhanced fluorescence (MAMEF) to detect low concentrations of target DNA in exosporium previously extracted from the surface of *B. anthracis* spores within 30 s.<sup>7</sup> The MAMEF technique integrates fluorescence surface assays on particulate plasmon-supporting metal substrates, with low-power microwave heating, to amplify fluorescence signatures and kinetically accelerate bimolecular recognition events, respectively. While the presence of a *B. anthracis* specific DNA signature on the surface of a spore is rapidly detected,<sup>7</sup> the quantity of target DNA can be highly variable depending on how the spore is prepared and processed.<sup>7</sup>

The release of DNA from a *B. anthracis* spore is arduous and time-consuming with current approaches for the most part failing to deliver the required rapidity and sensitivity. Various methodologies have been adopted to release DNA from within the spore, including autoclaving,<sup>8,9</sup> sonication,<sup>10,11</sup> bead beating,<sup>6</sup> germina-

\* To whom correspondence should be addressed. E-mail: geddes@umbi.umd.edu.

<sup>†</sup> Institute of Fluorescence, Laboratory for Advanced Medical Plasmonics and Laboratory for Advanced Fluorescence Spectroscopy, University of Maryland Biotechnology Institute.

<sup>‡</sup> Biodefense Initiative, University of Maryland Biotechnology Institute.

<sup>§</sup> Cardiff University.

(1) Baillie, L.; Read, T. D. *Curr. Opin. Microbiol.* **2001**, *4*, 78–81.

(2) Baillie, L. W. J. *J. Appl. Microbiol.* **2006**, *101*, 594–606.

(3) Smith, H.; Keppie, J. *Nature* **1954**, *173*, 869–870.

(4) Almeida, J. L.; Wang, L. L.; Morrow, J. B.; Cole, K. D. *J. Res. Natl. Inst. Stand. Technol.* **2006**, *111*, 205–217.

(5) Ellerbrok, H.; Nattermann, H.; Ozel, M.; Beutin, L.; Appel, B.; Pauli, G. *FEMS Microbiol. Lett.* **2002**, *214*, 51–59.

(6) Reif, T. C.; Johns, M.; Pillai, S. D.; Carl, M. *Appl. Environ. Microbiol.* **1994**, *60*, 1622–1625.

(7) Aslan, K.; Zhang, Y.; Hibbs, S.; Baillie, L.; Previte, M. J.; Geddes, C. D. *Analyst* **2007**, *132*, 1130–1138.

(8) Dang, J. L.; Heroux, K.; Kearney, J.; Arasteh, A.; Gostomski, M.; Emanuel, P. A. *Appl. Environ. Microbiol.* **2001**, *67*, 3665–3670.

(9) Fasanella, A.; Losito, S.; Adone, R.; Ciuchini, F.; Trotta, T.; Altamura, S. A.; Chiocco, D.; Ippolito, G. *J. Clin. Microbiol.* **2003**, *41*, 896–899.

(10) Chandler, D. P.; Brown, J.; Bruckner-Lea, C. J.; Olson, L.; Posakony, G. J.; Stults, J. R.; Valentine, N. B.; Bond, L. J. *Anal. Chem.* **2001**, *73*, 3784–3789.

(11) Luna, V. A.; King, D.; Davis, C.; Rycerz, T.; Ewert, M.; Cannons, A.; Amuso, P.; Cattani, J. J. *J. Clin. Microbiol.* **2003**, *41*, 1252–1255.

tion,<sup>6</sup> and chemical treatment.<sup>12</sup> Luna and colleagues<sup>11</sup> compared the effectiveness of a number of these approaches and concluded that heat shock followed by sonication and autoclaving prior to PCR was the most sensitive approach, being able to detect less than 10 spores in a sample. Unfortunately, this multistep process is both labor intensive and time-consuming, taking several hours to generate a result.

As an alternative to these methodologies, a low-power, low-cost, microwave-based approach that utilizes centimeter-sized metal disjoined "bow-tie" structures to focus the microwaves onto a desired structure, such as a bacterium or spore, has been developed.<sup>13,14</sup> A 20-s focused microwave burst was found to be sufficient to induce morphological changes in both vegetative organisms and spores as demonstrated by Transmission Electron Microscopy (TEM). Gel electrophoresis methods were used to confirm that irradiation resulted in the release of DNA from the spores. Further demonstration of the detection of less than 50 vegetative organisms per sample, within 60 s total time (preparation and detection time) were accomplished by combining the focused microwave approach and the MAMEF platform technology.

## MATERIALS AND METHODS

**Bacterial Strains and Probes.** The Sterne, 34F2 strain of *B. anthracis*, an attenuated variant employed extensively as an animal vaccine, a germination deficient variant ( $\Delta$ gerH) of *B. anthracis* Sterne 34F2<sup>15</sup> and the *Bacillus cereus* type strain ATCC 14579,<sup>16</sup> were obtained from the Biological Defense Research Directorate, Naval Medical Research Center, Silver Spring, MD. Difco L agar and Difco L broth were obtained from Becton Dickinson and Co. (Becton Drive, Franklin Lakes, NJ) and made up as per the manufacturers' instruction. *CAUTION: All work involving non-virulent spores and vegetative cells of bacterial strains should be carried out in a Class II Biological Safety Cabinet.*

The anchor and fluorescent probes for a highly conserved region within the gene encoding the protective antigen (PA) were designed according to the sequence published by Welkos et al.<sup>17</sup> and are given elsewhere.<sup>18</sup>

**Production of Spores.** Spores of a germination deficient variant ( $\Delta$ gerH) of *B. anthracis* Sterne 34F2 and the *B. cereus* type strain ATCC 14579 were prepared as previously described.<sup>19</sup>

**Preparation of Vegetative Organisms.** Vegetative organisms (PA-proficient and PA-deficient strains) were prepared from a single colony that was inoculated in 300 mL of LB broth A and incubated at 37 °C (shaking, 250 rpm) until the OD 600 nm reached  $0.400 \pm 0.01$ . Cultures were centrifuged at 4200g for 10

min at 4 °C and resuspended in 5 mL of PBS (pH 7.2) to achieve an approximate density of  $1 \times 10^9$  cfu mL<sup>-1</sup>. Stock solutions of cultures were prepared to an approximate final concentration of  $1.0 \times 10^7$  cfu mL<sup>-1</sup>.

**Extraction of DNA from *B. anthracis* Spores and Vegetative Organisms Using a DNA Extraction Kit in the Absence of Microwave Irradiation.** DNA was extracted from 500  $\mu$ L of stock solutions of spores and vegetative organisms using a commercially available DNA extraction protocol (Gentra Puregene by Qiagen), whereby the cells were resuspended in lysis solution with lytic enzyme and incubated at 37 °C for 30 min. The lysed spores and vegetative organisms were pelleted, and the resultant supernatant was saved. Subsequently, the total DNA was released from the spores and vegetative organisms by pipetting and resuspending the pellet in lysis solution. The suspension solution was treated with RNase A and protein precipitation solution, the precipitated proteins were pelleted, and the resultant supernatant was added to 2-propanol to precipitate the total DNA (Figure 4a). The total DNA was resuspended in 50  $\mu$ L of DNA hydration solution (included in the Gentra Puregene DNA extraction kit), and 20  $\mu$ L was run on a 0.8% agarose gel.

**Extraction of DNA from *B. anthracis* Spores and Vegetative Organisms Using Focused Microwave Irradiation.** *B. anthracis* spores and vegetative organisms were exposed to microwave irradiation in the presence of the bow-tie structures. For focused microwave extraction procedures, 500  $\mu$ L of stock spore ( $1.0 \times 10^7$  spores/mL) or vegetative organisms ( $\sim 1.0 \times 10^7$  cfu mL<sup>-1</sup>) was spun down and resuspended in 50  $\mu$ L of lysis solution. The concentrated spore culture was subjected to 20-s microwave pulses, and the resultant sample contents were resuspended in 500  $\mu$ L of lysis solution. The lysed spore and vegetative organism contents were pelleted and the supernatants were spared. The pelleted cells were also resuspended in PBS buffer. The remaining DNA extraction steps (RNase treatment, protein precipitation, and 2-propanol precipitation) were performed on the supernatant and the pelleted cells and subsequently used in gel electrophoresis (Figure 4a).

**Gel Electrophoresis.** Agarose gels were prepared at 0.8% in Tris acetate-EDTA buffer and run at 80 V on a Sub-Cell GT agarose gel electrophoresis system (Bio Rad Laboratories).

**Deposition of Aluminum Triangles on Glass Substrates To Lyse *B. anthracis* Spores and Vegetative Organisms.** Glass microscope slides were covered with a mask (an aluminum foil cut with a razor blade, 12.5 mm in size) to leave a triangular bow-tie region exposed. Equilateral aluminum triangles of 12.5-mm size (thickness 75 nm) were deposited onto a glass microscope slide using a BOC Edwards 306 vacuum deposition system. A self-adhesive silicon isolator (1 cm in diameter) was placed on top of the aluminum triangles' bow-tie region.

**Formation of Silver Island Films (SiFs) on Glass Substrates.** SiFs were prepared according to the procedure published previously.<sup>20</sup>

**Procedure for DNA Extraction with Focused Microwaves for the MAMEF Assays.** Fifty microliters of the spores ( $10^7$  spores/mL of spores) or vegetative organisms (various concentrations) was placed inside the silicon isolator and was covered with a thin coverslip. These samples were then heated up to 20 s in a

(12) Kuske, C. R.; Banton, K. L.; Adorada, D. L.; Stark, P. C.; Hill, K. K.; Jackson, P. J. *Appl. Environ. Microbiol.* **1998**, *64*, 2463-2472.

(13) Preville, M. J. R.; Geddes, C. D. *J. Fluoresc.* **2007**, *17*, 279-287.

(14) Preville, M. J.; Aslan, K.; Geddes, C. D. *Anal. Chem.* **2007**, *79*, 7042-7052.

(15) Weiner, M. A.; Read, T. D.; Hanna, P. C. *J. Bacteriol.* **2003**, *185*, 1462-1464.

(16) Ivanova, N.; Sorokin, A.; Anderson, I.; Galleron, N.; Candelon, B.; Kapatral, V.; Bhattacharyya, A.; Reznik, G.; Mikhailova, N.; Lapidus, A.; Chu, L.; Mazur, M.; Goltsman, E.; Larsen, N.; D'Souza, M.; Walunas, T.; Grechkin, Y.; Pusch, G.; Haselkorn, R.; Fonstein, M.; Ehrlich, S. D.; Overbeek, R.; Kyrpides, N. *Nature* **2003**, *423*, 87-91.

(17) Welkos, S. L.; Lowe, J. R.; Edenmccutchan, F.; Vodkin, M.; Leppla, S. H.; Schmidt, J. J. *Gene* **1988**, *69*, 287-300.

(18) Aslan, K.; Zhang, J.; Preville, M. J. R.; Baillie, L.; Hibbs, S.; Geddes, C. D. *Analyst* **2007**, *132*, 1130-1138.

(19) Baillie, L.; Hibbs, S.; Tsai, P.; Cao, G. L.; Rosen, G. M. *FEMS Microbiol. Lett.* **2005**, *245*, 33-38.

(20) Aslan, K.; Geddes, C. D. *Anal. Chem.* **2005**, *77*, 8057-8067.

microwave cavity (a 0.7 cu ft, GE Compact microwave model JES735BF, maximum power 700 W, duty cycle of 2 is used).

**Preparation of the MAMEF Assay Platform for the Ultrafast Detection of DNA Extracted from *B. anthracis* Spores and Vegetative Organisms.** The detailed experimental procedure was described previously.<sup>18</sup> Here, the importance of several crucial technological steps is emphasized. The nonspecific binding of target DNA and fluorescent probe to the parts of the glass slides not covered by silver nanoparticles, and on silver nanoparticles themselves, was prevented with succinic anhydride and amino-(ethoxy)ethanol, respectively. Silicon isolators containing wells (5 mm in diameter) were applied onto the MAMEF assay platform to create wells that can hold samples up to 50  $\mu\text{L}$ .

**MAMEF-Based DNA Assays Using a Microwave Cavity.** The MAMEF DNA assay has been described in detail previously.<sup>7</sup> In summary, a solution containing anthrax DNA was mixed with a fluorophore-labeled oligonucleotide (fluorescent probe) and was then microwave heated on SiF surfaces that contained an anchor probe specific to anthrax DNA for 30 s. The temperature gradient, created by the selective heating of solution (warmer) over silver nanoparticles (colder), drives the DNA samples toward the colder SiFs, where the hybridization rapidly takes place. Moreover, heat provided by the microwaves is thought to lower the activation energy of the hybridization process and has been described by us elsewhere.<sup>7,21</sup>

In this study, MAMEF-based DNA capture assay was performed by the incubation of the solution containing spores or vegetative organisms (immediately after the microwave exposure) mixed with TAMRA-labeled fluorescent probe in Hepes buffer (Supporting Information, Figure 3) for 30 s in a microwave cavity. The total time of the assay was 1 min (exposure of spores to focused microwaves, 20 s + transfer of sample and mixing with the fluorescent probes on SiFs, 10 s + DNA hybridization on SiFs with microwave heating, 30 s). In order to determine the extent of nonspecific binding of target DNA mixed with TAMRA-labeled fluorescent probe, an aliquot of the mixture was incubated on the SiF surface without the thiolated anchor probe for 30 s in a microwave cavity (GE compact microwave). Experiments pertaining to the nonvirulent strain *B. cereus* were performed in the same way. The power setting of the microwave cavity was set to 2. In all the experiments performed with low-power microwaves using the SiF surface, there was no evidence of sample drying, which was accomplished by using the "blackbody" concept introduced in a previous publication,<sup>20</sup> as well as by the spacing of the triangles themselves.<sup>14</sup>

**Finite-Difference Time-Domain (FDTD) Simulations.** Detailed descriptions of the FDTD simulation for disjointed bow-tie structures have been previously described by us.<sup>14</sup> Electric field distributions are normalized with respect to the maximum electric field intensity in the  $x$ - $y$  image plane.

**Thermal Imaging Setup and Experimental Conditions.** Thermal imaging is accomplished using the following procedure: a 1-in.-diameter opening was cut through the bottom of the microwave cavity, and all exposed metal surfaces were coated with white enamel reflective paint. Sapphire plates (Swiss Jewel), 1-in. diameter and 1 mm thick, were placed above the cavity opening

as sandwich geometries to thermally image the temperature distributions of the glass and aluminum triangle samples, whereby 250  $\mu\text{L}$  of water is dropped on a blank sapphire plate and the substrates are placed on another sapphire plate to create a sandwich. For the glass substrates with the aluminum triangles, the samples were inverted such that the bow-tie structures were in contact with the water. Infrared emission from the sample geometry in the microwave cavity was imaged by reflecting the radiation from a gold mirror onto a thermal imaging camera (Silver 420M; Electrophysics Corp., Fairfield, NJ) that was equipped with a closeup lens, providing a resolution of  $\sim 300 \mu\text{m}$ .

Images were collected at 50 Hz for 20 s. Samples were exposed to 2-s microwave pulses that were applied immediately following the commencement of thermal image collection. Timing graphs are reflective of the mean intensity temperature over the entire area of the respective outlined regions. Since initial sample temperatures were slightly variable, the temperature timing graphs are normalized with respect to the initial temperature of the respective samples. These values are then appropriately scaled to reflect the relative change in temperature of the surfaces. Example thermal images are true temperature images that correlate with discrete time points of the overall image collection time.

**Transmission Electron Microscopy.** TEM were taken with a side-entry electron microscope (JEOL Jem 1200 Ex II microscope). Samples were cast from water solutions onto standard carbon-coated (200–300 Å) Formvar films on copper grids (200 mesh) by placing a droplet of a 5- $\mu\text{L}$  aqueous sample solution on a grid, waiting 5 min, and removing excess solution by touching a small piece of filter paper to the edge of the grid. The grid was dried in air for 24 h.

**Fluorescence Spectroscopy.** All fluorescence assay measurements were performed by collecting the emission intensity through a long-pass filter (532 nm) perpendicular to the assay surface, after total-internal reflection (a standard prism) evanescent wave excitation, using a 532-nm diode laser and a fiber-optic spectrometer (HD2000) from Ocean Optics, Inc. The optical configuration was assembled using components that are commercially available and is used in many publications.<sup>22</sup>

## RESULTS AND DISCUSSION

**Design of Aluminum Disjointed Bow Ties to Highly Focus Microwave Energy.** When exposed to 2.45-GHz microwave irradiation in a conventional microwave cavity, large electric field distributions at the gap of 12.5-mm aluminum disjointed bow-tie geometries were recently demonstrated (Figure 1a).<sup>14</sup> Previously, this technology was implemented to accelerate enzymatically and chemically catalyzed reactions.<sup>13,14</sup> In those experiments, the increased heating rates for solutions in proximity to the disjointed bow-tie gaps were also calculated. In light of these observations, the disjointed bow-tie geometry is now adopted to explore the effects of focused microwave radiation on *B. anthracis* spores (Figure 1b).

Prior to the irradiation of *B. anthracis* with focused microwaves, the real-time temperature changes of water sandwiched between a sapphire plate and a blank glass slide (a control

(21) Aslan, K.; Malyn, S. N.; Geddes, C. D. *Biochem. Biophys. Res. Commun.* **2006**, *348*, 612–617.

(22) Matveeva, E.; Gryczynski, Z.; Malicka, J.; Gryczynski, I.; Lakowicz, J. R. *Anal. Biochem.* **2004**, *334*, 303–311.



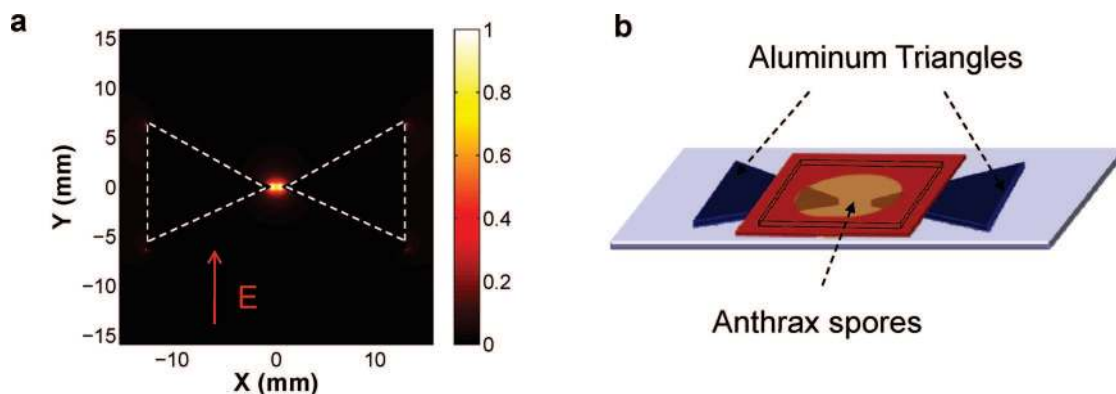


**Figure 1.** (a) Normalized FDTD simulation of field intensity distributions ( $|x + ly|$ ) for equilateral aluminum triangles in a simulated 2.45 GHz transverse electric polarized total-field scattered field (TFSF) that propagates across the geometries from bottom to top. (b) A schematic representation of the experimental setup used to release DNA from *B. anthracis* spores and the vegetative organisms. Equilateral aluminum triangles of 12.5 mm size (thickness 75 nm) are deposited onto a glass microscope slide. The gap between the two triangles is 1 mm and is covered with a 1 cm square silicon well. *B. anthracis* spores and vegetative organisms dispersed in buffer (volume 250  $\mu\text{L}$ ) are microwave heated inside the silicon well for 20 s, and a glass coverslip is used to cover the liquid.

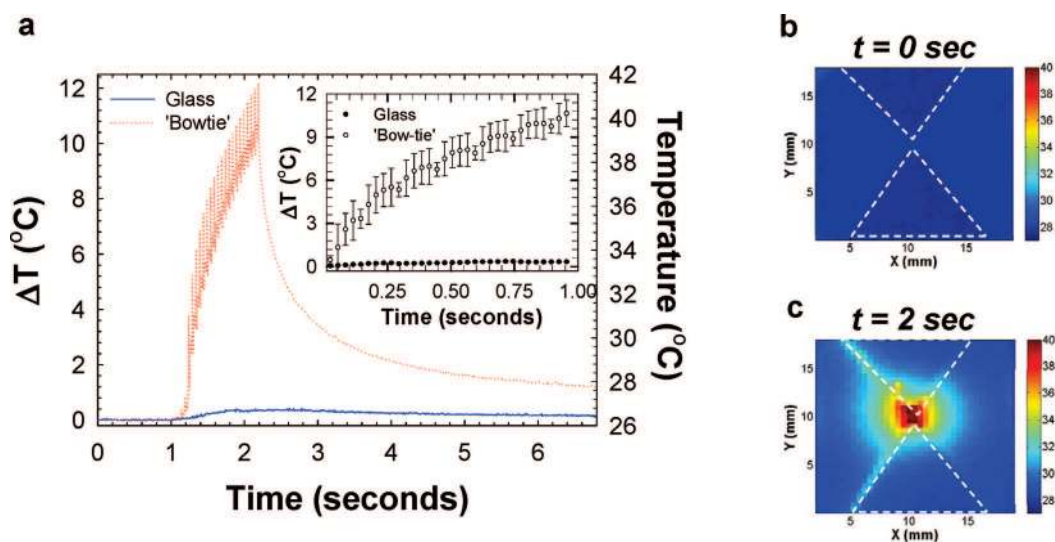


**Figure 2.** (a) Change in temperature ( $\Delta T$ ) vs time, for water on a glass slide (denoted as glass, solid line) and on a glass slide modified with equilateral aluminum triangles (denoted as bow tie, dotted line), recorded using a thermal imaging camera. A sapphire plate was placed between the thermal imaging camera and water for accurate temperature measurements. The initial temperature was 26  $^{\circ}\text{C}$  in both cases. Microwave heating initiated at  $t = 1$  s. Inset: Initial change in temperature after the initiation of microwave heating. (b, c) Thermal images of bow-tie aluminum structures before ( $t = 0$  s) and after ( $t = 2$  s) microwave heating. Duty cycle of microwave cavity is 1 s.

sample) or a glass slide modified with the disjointed bow-tie geometry was monitored using a thermal imaging camera to assess the temperature rise in the experimental setup.<sup>23</sup> From the temperature versus time plots, the temperature of water on a blank glass slide increases and was observed to be only 0.5 and 2  $^{\circ}\text{C}$ , and the temperature of water between aluminum triangles increases was 12 and 30  $^{\circ}\text{C}$  in 1 and 2 s (duty cycle) of microwave irradiation, respectively (Figure 2a and Supporting Information, Figure 1), indicating the significant temperature jumps in the gap of the bow-tie geometries within seconds. Thermal images of the temperature distributions in the presence of aluminum triangles illustrate the temperature distributions in the presence of disjointed bow-tie geometries both before and after exposure to microwave irradiation (Figure 2b, c, respectively). The temperature increase between triangles

captured by the thermal imaging camera correlates well with electric field distributions predicted for 2.45-GHz simulated TFSF incident on disjointed 12.5-mm bow-tie geometries with a 1-mm gap size (Figure 1a).

**Release of DNA from Spores Using Aluminum Bow Ties and Focused Microwaves.** With the focused microwave energy and subsequent rapid heating of the solutions in the gaps of the disjointed bow-tie geometries, this technology was employed as an alternative to the complex and long incubation periods typically required for releasing DNA from *B. anthracis* spores using current technologies. In this regard, a small volume (50  $\mu\text{L}$ ) of spores ( $1.0 \times 10^5$  spores/mL) was placed in the gap of the aluminum triangles (Figure 1b) and was irradiated for 20 s in a microwave cavity in the presence and absence of the disjointed bow-tie geometry.

Using TEM, the morphological changes of the spores after 20 s of microwave heating on a blank glass microscope slide

(23) Previte, M. J.; Zhang, Y.; Aslan, K.; Geddes, C. D. *J. Fluoresc.* **2007**, *17*, 639–642.

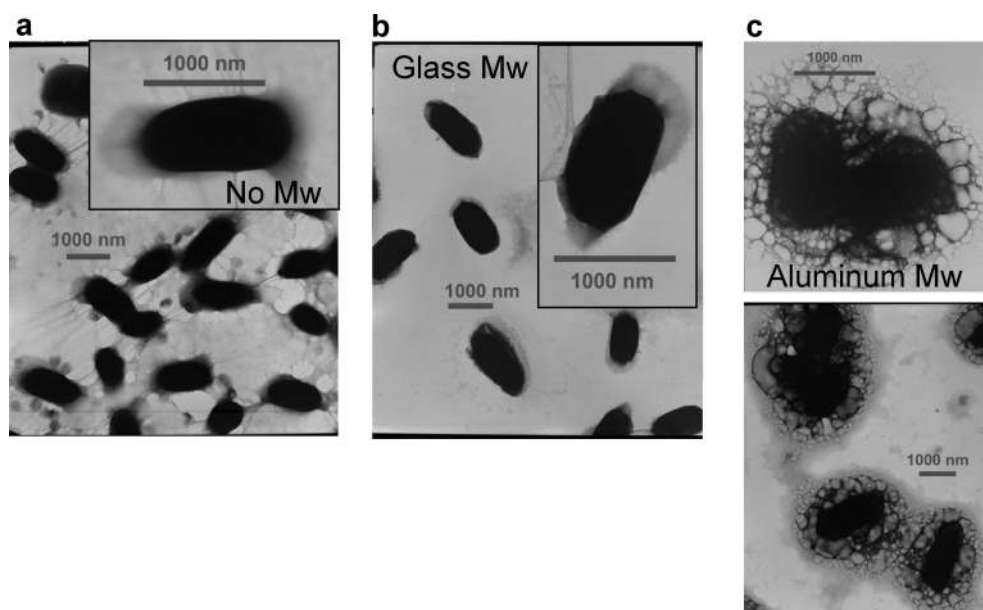


**Figure 3.** Transmission electron micrograph images of *B. anthracis* spores (a) before, (b) on glass, and (c) on aluminum triangles after 20 s of low-power microwave heating. While microwave heating on glass slides does not appear to cause any structural change in the spores, microwave heating of spores from between the aluminum triangles results in the rapid deformation of the spore and the release of DNA. No Mw, no microwave heating; Mw, microwave heating.

and on aluminum triangles was compared (Figure 3). *B. anthracis* form elongated rod-shaped spores ~1000 nm in length, which are surrounded by a structure called the exosporium (transparent membrane around the spores (Figure 3a). During microwave heating of the spores in the absence of the disjointed bow-tie geometry, no obvious structural changes in the spore and the exosporium were observed (Figure 3b). However, in the presence of the disjointed bow-tie antennas, a significant morphological change to the exosporium was seen while the changes in the cortex of the spores were more subtle (Figure 3c). Similarly, exposure of the vegetative organisms to microwave heating resulted in cellular disruption (see Supporting Information, Figure 2b).

The TEM images provided the visual evidence for the physical disruption of the spore and the vegetative organisms and the potential release of DNA using focused microwave heating. From the TEM images, the DNA release was initially thought to be from the core and the exosporium of the vegetative organisms and the spores, respectively. To determine if this is indeed the case, a qualitative evaluation of the release of DNA following focused microwave heating was undertaken using a gel electrophoresis technique. Two subsequent DNA extraction methodologies were performed on native cultures and those exposed to focused microwave irradiation (Figure 4a). Extract 1 was performed to isolate genomic DNA released into suspension buffer after organisms were lysed (Figure 4a, step 5a). Extract 2 was performed to isolate DNA that was released from organisms subsequent to microwave irradiation (Figure 4a, step 4). The extracted DNA was analyzed using gel electrophoresis as follows: (sample A) DNA extract 1 (lane 3) and extract 2 (lane 4) from samples of vegetative organisms that were not exposed to focused microwave irradiation; (sample B) DNA extract 1 (lane 5) and extract 2 (lane 6) from samples of vegetative organisms that were exposed to focused microwave irradiation; (sample C) DNA extract 1 (lane 7) and extract 2 (lane 8) from samples of spores

that were not exposed to focused microwave irradiation; (sample D) DNA extract 1 (lane 9) and extract 2 (lane 10) from samples of spores that were exposed to focused microwave irradiation.

From the gel results (Figure 4) showed that the DNA extraction protocol performed on irradiated and nonirradiated vegetative organisms generated DNA extract 1 yields were qualitatively similar based on the intensity of the bands (sample A, lane 3 and sample B, lane 5, respectively). For both samples A and B, no DNA yields from the extraction 2 protocol were observed (sample A, lane 4 and sample B, lane 6). DNA extraction procedures performed on nonirradiated spores failed to yield any detectable DNA, suggesting that the DNA extraction protocol that was used was unable to break open *B. anthracis* spores (lanes 7 and lane 8). In contrast, the DNA extraction procedure 1 performed on microwave-irradiated spores did yield DNA. As a consequence of disruption of the exosporium, our results indicate that irradiating spores with focused microwave energy resulted in the release of DNA, which was subsequently detected using extraction protocol 2 (Figure 4, lane 10). These results confirm that DNA recovered from the *B. anthracis* spores originates from the cortex of the spore as the exosporium is disrupted by the microwave heating (Figure 3). In contrast, the DNA recovered from the vegetative organisms is from the cells themselves as these organisms lack the exosporium.

The reason that the use of enzymatic DNA extraction protocol (no exposure to focused microwave irradiation) did not yield any detectable levels of DNA from *B. anthracis* spores is thought to be due to the inability of the commercially available DNA extraction reagents to disrupt the outer cortex of the spores. In contrast, DNA was recovered from *B. anthracis* spores which were exposed to 20 s of focused microwave irradiation. Due to the dramatic differences in the dielectric properties of spores and the vegetative organisms, it is possible that the exosporium of the spores more effectively absorbs microwave irradiation. From the TEM images, it is clearly evident that the exosporium is locally heated creating cavitations. Since the

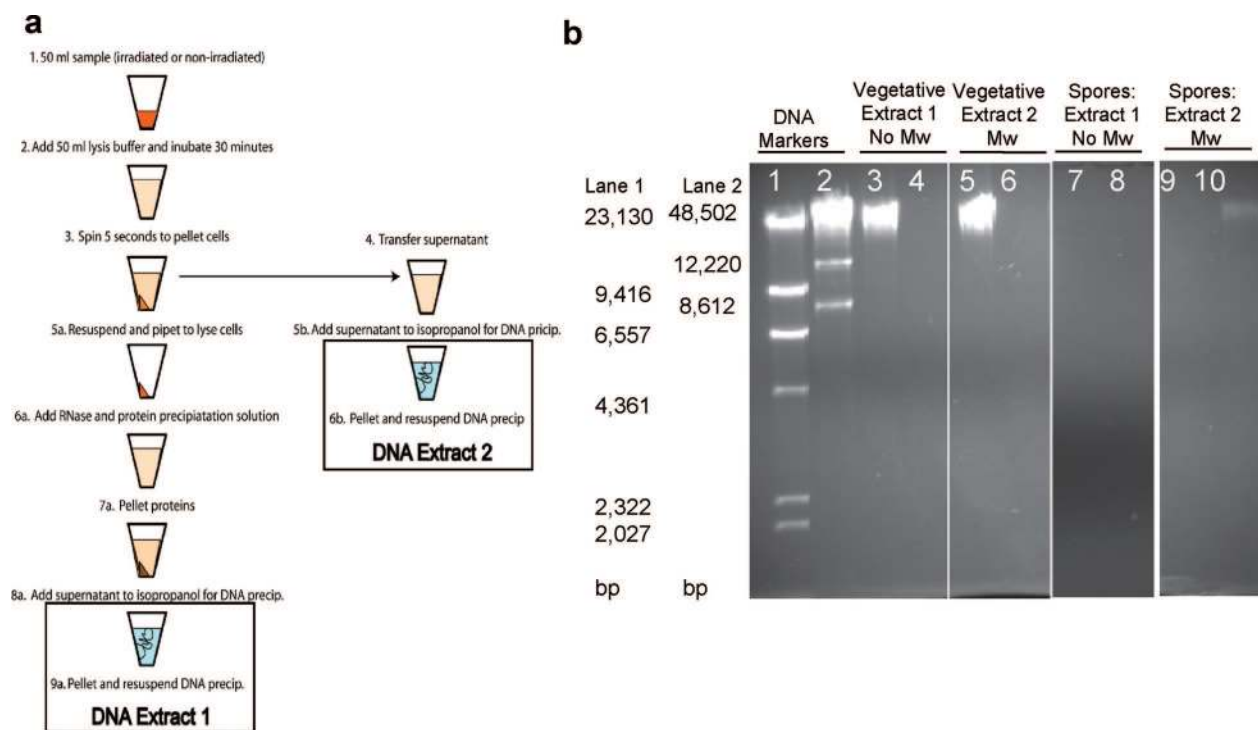


**Figure 4.** (a) Flow diagram of DNA extraction procedures (DNA extract 1 and extract 2) for irradiated and nonirradiated vegetative organisms and spore cultures. (b) Lanes: 1.  $\lambda$ /HindIII marker. 2. High molecular weight. 3. DNA extracted from vegetative organisms (sample 1). 4. DNA extraction from supernatant of vegetative organisms (sample 1). 5. DNA extracted from vegetative organisms exposed to  $3 \times 5$  s microwave pulses in the presence of disjoined bow-tie antenna (sample 2). 6. DNA extracted from supernatant of vegetative organisms exposed to  $3 \times 5$  s microwave pulses in the presence of disjoined bow-tie antenna (sample 2). 7. DNA extracted from *B. anthracis* spores and exposed to  $3 \times 5$  s microwave pulses in the presence of disjoined bow-tie antenna (sample 3). 8. DNA extracted from *B. anthracis* spores from supernatant of spores lysed after microwave irradiation and treatment with lytic enzyme solution (sample 3). 9. DNA extracted from *B. anthracis* spores (sample 4). 10. DNA extracted from supernatant of *B. anthracis* spores (sample 4). Lanes 9 and 10 were run on a gel different from lanes 1–8.

water-based exosporium has a large dielectric constant compared to the dehydrated high carbon content of the cell wall of the organisms, it is likely that localized heating of the exosporium concentrates the heating of the spore's cortex, which facilitates the subsequent release of the DNA from the core. The gel results show that the total DNA released from the spores and vegetative cells were mostly larger than 48 000 base pairs. Although the presence of DNA with smaller size is not evident from the gel results due to very intense band for larger DNA, the sample is likely to contain smaller DNA.

It is important to comment on the extent of potential DNA damage due to microwave heating of the samples. Two possible mechanisms can potentially cause damage to DNA: (1) temperature and (2) focused electric fields. The fact that the temperature increase of the solution is only  $\sim 30$  °C (for a 2-s microwave duty cycle), the DNA extracted from the spores or vegetative cells is thought to melt to some extent, and the temperature was not high enough. Although, not studied here, it is possible that the increased electric fields between the aluminum triangles can also cause DNA damage due to the electric conductivity of DNA.<sup>24,25</sup>

**Microwave-Accelerated Detection of DNA Using the MAMEF Platform Technology.** The application of the MAMEF platform technology to the ultrafast and sensitive detection of fluorophore-labeled target DNA sequences was previously re-

ported.<sup>21</sup> The applicability of the MAMEF technology to a three-piece DNA detection scheme whereby a silvered glass slide is modified with an anchor probe and a target DNA sequence is detected with a fluorescence probe in less than 30 s was also demonstrated. In this scheme, the anchor probe and the fluorescent probe hybridize with different regions of the target DNA in proximity to the silver surface, where the fluorescence emission is plasmon-enhanced, ultimately yielding an increased assay sensitivity (Also see Supporting Information, Figure 3).<sup>7</sup> In addition, silvered surfaces preferentially focus microwave energy, providing us with ultrafast DNA hybridization kinetics.<sup>20,21</sup>

In this paper, the MAMEF-based three-piece DNA detection scheme (Supporting Information, Figure 3)<sup>7</sup> was adapted to detect DNA released from *B. anthracis* following exposure to focused microwave irradiation. To determine the effectiveness of this approach, the following samples were assayed: (A) *B. anthracis* spores without microwave heating (room temperature assay); (B) *B. anthracis* spores exposed to microwave irradiation on a blank glass microscope slide; and (C) *B. anthracis* spores exposed to focused microwave irradiation between aluminum triangles. Control experiments were also performed, whereby the anchor probe was omitted from the metal surface (cf. Supporting Information, Figure 3). These control experiments demonstrated the extent of nonspecific binding of target DNA to the assay surface (Figure 5). Incubation of *B. anthracis* spores at room temperature in the presence of a fluorescent probe specific for the PA gene of *B. anthracis* located on the MAMEF assay platform, in the absence

(24) Cohen, H.; Noguez, C.; Uilien, D.; Daube, S.; Naaman, R.; Porath, D. *Faraday Discuss.* **2006**, *131*, 367376, 393–402.

(25) Cohen, H.; Noguez, C.; Naaman, R.; Porath, D. *Proc. Natl. Acad. Sci. U. S. A.* **2005**, *102*, 11589–11593.



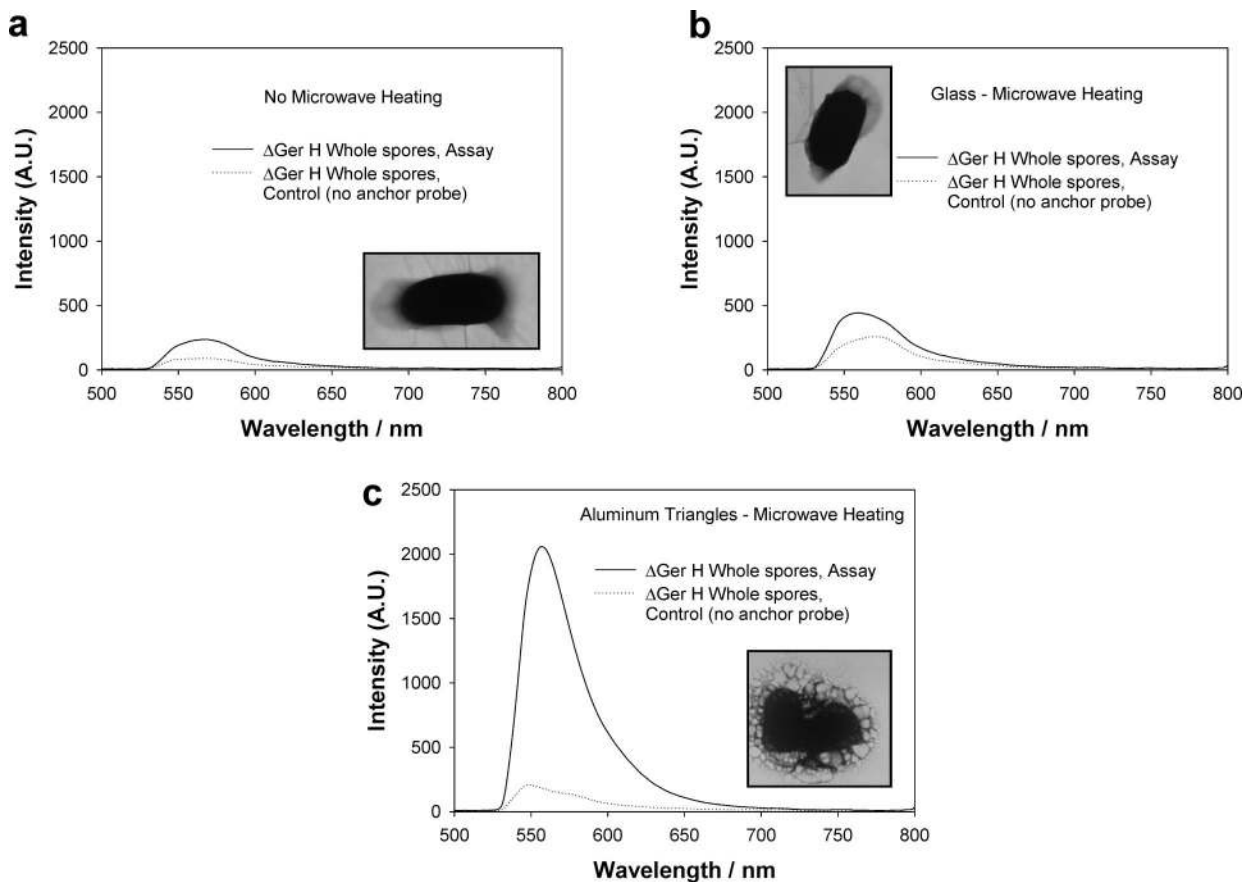


**Figure 5.** (a) Room-temperature assay and (b, c) MAMEF assays for *B. anthracis* spores. *B. anthracis* spores ( $10^5$  spores/mL) were microwave heated for 20 s on the MAMEF assay, and the same number of spores were also incubated on the assay platform for 2 h without microwave heating in the room temperature assay. The anchor probe is omitted in the control assays. A.U., arbitrary fluorescence units.

of microwave heating, resulted in a fluorescence emission signature similar to that of a control assay (where the anchor probe was omitted) (Figure 5a).

Exposure of spores to microwave irradiation for 20 s at room temperature on glass resulted in a slightly higher fluorescence emission when run on the assay, but again, it is indistinguishable from its corresponding control sample assay (no anchor probe) (Figure 5b). In the MAMEF assay for *B. anthracis* spores, which were exposed to focused microwave irradiation between aluminum triangles, a significantly larger fluorescence emission signature was observed (Figure 5c). This implies that the sample containing anthrax DNA after the exposure to focused microwave heating is detected by the MAMEF assay. To ensure the specificity of the assay, spores of the genetic close relative *B. cereus* were exposed to microwave heating also between aluminum triangles. Following irradiation, the treated spores were mixed with the fluorescent probe and irradiated for a further 20 s (Supporting Information, Figure 4). We observed an  $\sim 4$ -fold lower fluorescence emission intensity from the MAMEF assay for *B. cereus*, as compared to the MAMEF assay for *B. anthracis*. This is due to the fact that the MAMEF assay components are specifically designed are specific for *B. anthracis*.

Next, the ability of the MAMEF technique to detect the vegetative organisms themselves was studied (Figure 6 and Supporting Information, Figure 5). It is important to note that the data collected for spores and vegetative cells are for the proof-of-principle demonstration of the applicability of the technique to

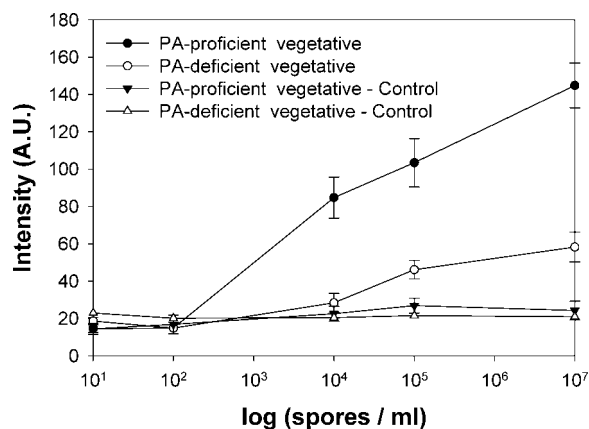


**Figure 6.** MAMEF assays for vegetative organisms. Vegetative organisms were microwave heated for 20 s and were then used in the assay. The anchor probe was omitted on the control assays. A.U., fluorescence arbitrary units.

both sample types and are not directly comparable. As a further confirmation of the specificity of the assay, an isogenic variant of *B. anthracis* that lacked the PA gene (labeled as PA-deficient vegetative in Figure 6) was included. A concentration-dependent fluorescence emission from the vegetative *B. anthracis* cultures (labeled as PA-proficient vegetative in the Figure 6) was observed to be significantly larger than the fluorescence emission from the PA-deficient vegetative *B. anthracis* variant when the irradiated vegetative cultures are mixed with the fluorescent probe and are

incubated on the MAMEF assay platform for 20 s. The control experiments, where the anchor DNA probe is omitted from the surface of the MAMEF assay platform, showed a minimal background fluorescence emission (signal-to-noise ratio of 7). Using this approach, the detection limit of much less than 1000 vegetative cells/mL was achieved (Supporting Information, Figure 5).

It is also important to comment on the potential real-world usage of the techniques presented here. At this time, the authors believe that the application of these techniques to real-world samples, which can be carried out by trained specialists in centralized laboratories, is fairly easy. Since clinical samples (specifically serum and blood) are amenable to microwave processing,<sup>26–28</sup> one can expect that the short exposure to focused microwave bursts employed here to extract DNA from spores or vegetative cells can be also be carried out with clinical samples. Although, the final evaluation of the presence of anthrax DNA still requires advanced tools, the development of simpler detection systems, similar those used in point-of-care devices, would certainly afford the flexibility needed for a fast response in the case of a biological terror attack.

## CONCLUSIONS

In this work, the successful amalgamation of microwave energy and the metal-enhanced fluorescence technology for the ultrafast detection of *B. anthracis* spores, through theoretical calculations

and low-cost experimental geometries and procedures, was demonstrated. For the first time, it was shown that *B. anthracis* DNA can be extracted from spores and subsequently detected with minimal preprocessing steps in under 1 min total time. In this regard, disjoined bow-tie metal structures were implemented to focus 2.45-GHz microwave energy in a conventional microwave cavity to induce the release of DNA from the *B. anthracis* spores. The permutation of *B. anthracis* spores and vegetative organisms and the release of DNA were confirmed by TEM analysis and gel electrophoresis, respectively, with more total DNA detectable using the approach presented here. DNA extracted from as low as 1000 organisms/mL was mixed with a fluorescent probe and captured on our MAMEF assay platform within a few seconds, where the fluorescence signal readout was readily detected. The MAMEF technology was also able to demonstrate high specificity and clearly distinguish between *B. anthracis* and *B. cereus*.

## ACKNOWLEDGMENT

This work was supported by the Middle Atlantic Regional Center of Excellence for Biodefense and Emerging Infectious Diseases Research (NIH NIAID U54 AI057168). Salary support to authors from UMBI, MBC, and the IoF is also acknowledged. K.A. and M.J.R.P. have contributed equally.

## SUPPORTING INFORMATION AVAILABLE

Additional information as noted in text. This material is available free of charge via the Internet at <http://pubs.acs.org>.

Received for review March 11, 2008. Accepted April 7, 2008.

AC800519R

(26) Armstrong, J. M.; Metherel, A. H.; Stark, K. D. *Lipids* **2008**, *43*, 187–196.

(27) Ozen, S.; Helhel, S.; Cerezci, O. *Burns* **2008**, *34*, 45–49.

(28) Aslan, K.; Malyn, S. N.; Geddes, C. D. *J. Immunol. Methods* **2007**, *323*, 55–64.